International Journal of Mass Spectrometry 306 (2011) 114–122

Contents lists available at ScienceDirect

International Journal of Mass Spectrometry

journal homepage: www.elsevier.com/locate/ijms

# DC potentials applied to an end-cap electrode of a 3D ion trap for enhanced $MS^n$ functionality

Boone M. Prentice[a], Wei Xu[b], Zheng Ouyang[b], Scott A. McLuckey[a,*]

[a] Department of Chemistry, Purdue University, West Lafayette, IN 47907, USA
[b] Weldon School of Biomedical Engineering, Purdue University, West Lafayette, IN 47907, USA

ARTICLE INFO

*Article history:*
Received 11 August 2010
Received in revised form
14 September 2010
Accepted 20 September 2010
Available online 29 September 2010

*Keywords:*
3D ion trap
Monopolar DC
Ion injection

ABSTRACT

The effects of the application of various DC magnitudes and polarities to an end-cap of a 3D quadrupole ion trap throughout a mass spectrometry experiment were investigated. Application of a monopolar DC field was achieved by applying a DC potential to the exit end-cap electrode, while maintaining the entrance end-cap electrode at ground potential. Control over the monopolar DC magnitude and polarity during time periods associated with ion accumulation, mass analysis, ion isolation, ion/ion reaction, and ion activation can have various desirable effects. Included amongst these are increased ion capture efficiency, increased ion ejection efficiency during mass analysis, effective isolation of ions using lower AC resonance ejection amplitudes, improved temporal control of the overlap of oppositely charged ion populations, and the performance of "broad-band" collision induced dissociation (CID). These results suggest general means to improve the performance of the 3D ion trap in a variety of mass spectrometry and tandem mass spectrometry experiments.



## 1. Introduction

Quadrupolar DC fields have been utilized in quadrupole ion traps (QIT) by applying a DC voltage to either the ring electrode or to both the exit and end-cap electrodes, with the DC voltage being of the same magnitude and polarity. Quadrupolar DC is generally used for ion isolation as it provides convenient means for manipulating the *a* parameter of the Mathieu stability diagram [1]. DC potentials can also be applied to a QIT in dipolar or monopolar fashion. This can be done, for example, either by applying a positive potential to the entrance end-cap electrode and a negative potential to the exit end-cap electrode (or vice versa), which is referred to a dipolar DC, or by applying a positive or negative potential to one end-cap while maintaining the other end-cap at ground, which is referred to as monopolar DC. The dipolar/monopolar DC potential influences ion motion in the plane of its application, in this instance the *z* direction. Selectively applying and removing DC voltages of varying magnitudes and polarities throughout a mass spectrometry experiment can provide for enhanced performance and control. Of particular interest here is the use of monopolar DC during time periods associated with ion accumulation, mass analysis, ion isolation, ion/ion reaction, and ion activation.

Weil et al. have performed simulations modeling the use of short (microsecond-long) DC pulses during ion injection and have observed increases in the capture efficiency of ions [2]. Several hundred volt attractive DC pulses were applied to the entrance end-cap electrode during appropriate phases of the RF cycle, timed to occur shortly following injection into the trap. These phase-locked pulses serve to minimize the kinetic energies of injected ions, thereby increasing the capture efficiency over short injection times. Similarly, March and Todd have discussed the use of such short, attractive DC pulses for ion trapping [1]. It has also been demonstrated that applying an attractive DC potential to the entrance end-cap electrode while also applying a repulsive DC potential to the exit end-cap during ion injection can increase the capture efficiency of high mass ions [3]. However, whether this phenomenon was due to a reduction in the kinetic energy of the ions by the applied potential to the exit end-cap or due to a focusing effect created by the entrance end-cap potential was unclear. Franzen et al. described a unique device that serves as a linear octapole trap during ion accumulation and as a 3D ion trap thereafter [4]. The ring electrode is divided into eight segments with alternating phases of an RF voltage applied to alternating segments. Following injection of the ions, the operation of the trap is switched back over to that of a 3D ion trap by applying a common RF phase to all segments. Operating the trap as a linear trap during ion accumulation allows for relatively efficient ion capture of the axially injected ions with low kinetic energies. In this case, both end-cap electrodes carry small repulsive DC voltages; however, these DC potentials are used primarily to trap ions in the axial dimension.

* Corresponding author at: 560 Oval Drive, Department of Chemistry, Purdue University, West Lafayette, IN 47907-2084, USA. Tel.: +1 765 494 5270; fax: +1 765 494 0239.
*E-mail address:* mcluckey@purdue.edu (S.A. McLuckey).

1387-3806/$ – see front matter © 2010 Elsevier B.V. All rights reserved.
doi:10.1016/j.ijms.2010.09.022

The use of dipolar DC in a 3D ion trap has also been described for mass-dependent ion ejection and for the transfer of ions to other devices. Fulford and March have shown the use of short DC pulses on one or both end-caps in characterizing the pseudopotential well depths for ions of varying $m/z$ [5]. Eizo has reported the use of kilovolt dipolar DC extraction potentials, termed ballistic ion extraction (BIE), in an ion trap time-of-flight (IT-TOF) set up [6]. In this arrangement, the ion trap serves as an ion source for the TOF. During extraction from the ion trap into the TOF, a repulsive kilovolt DC potential is applied to the entrance end-cap and an attractive kilovolt DC potential is applied to the exit end-cap while simultaneously lowering the RF ring voltage to 0 V. While this system uses kilovolt dipolar potentials, removes the RF ring voltage, and does not employ a mass-selective instability scan, it nonetheless demonstrates the principal of using dipolar DC to optimize ion extraction from the 3D trap. Michael et al. have reported similar results in an ion trap time-of-flight system [7]. DC pulses have also been used for transporting ions between traps in multiple ion trap arrangements [8,9].

The 3D ion trap has proved to be useful as a vessel for ion/ion reactions [10,11], whereby ions of opposite polarity are usually admitted sequentially into the ion trap and allowed to react. A complication in controlling the onset of reactions, however, arises from reactions that proceed while the second ion population is being accumulated. Control over ion/ion overlap can enable better definition of reaction initiation and could also allow for the isolation of ions admitted in the second ion accumulation period. Grosshans et al. have reported the use of dipolar DC in preventing ion/ion reactions as well as in controlling ion/ion reaction rates in ion parking experiments [12]. Ion parking refers to the inhibition of ion/ion reaction rates via minimizing overlap between oppositely charged ions and/or increasing the relative velocities of the reactants [13]. Single frequency resonance excitation can be used to inhibit the reaction rates of ions of narrow ranges of mass-to-charge ratio. Broad-band resonance excitation and the use of relatively high amplitude single frequency resonance excitation allow for the inhibition of wide ranges of mass-to-charge in a variation of ion parking referred to as 'parallel ion parking' [14]. Dipolar DC also can be used to effect parallel ion parking, as described by Grosshans et al. [12], by physically separating the cation and anion clouds in the $z$ direction. The extent of separation is determined in part by the trapping well-depths experienced by the ions under a given set of trapping conditions, which vary with the mass-to-charge ratios of the ions.

Dipolar DC also has been shown to be effective at performing collision-induced dissociation (CID) in a linear ion trap [15]. Conventional ion trap CID experiments employ a supplemental AC waveform, usually applied in dipolar fashion to both end-cap electrodes, in order to accelerate ions at their secular frequencies and induce energetic collisions with the background gas [16,17]. Relatively long DC pulses applied to the ring electrode have been used to bring ions close to the boundary of the stability diagram and induce CID [18]. Short DC pulses [19,20] and low frequency AC [21] also have been shown to cause CID in 3D ion traps. In these experiments, the dipolar DC acts to move the ion cloud to a new position in the pseudopotential well in the trap. The result is that the ions find themselves in an area of the pseudopotential well with increased potential energy. Multiple short pulses, both on and off, can be used in this manner to accelerate ions as they follow the changes in their positions in the pseudopotential well. The work reported here relies on the continuous application of monopolar DC over the millisecond to tens of milliseconds time-scales, which is analogous to the work of Tolmachev et al. using dipolar DC in a linear quadrupole ion trap [15]. The dipolar DC potential, applied across a rod pair in a linear ion trap, accelerates ions by shifting the ions to an area of higher RF field strength. This leads to RF heating of the parent ion and subsequent dissociation. The target gas mass, time scale over which the dipolar/monopolar DC is applied, the magnitude of the DC, and the low-mass cutoff (LMCO, which in part determines the pseudopotential well-depth) are important parameters in controlling the extent of dissociation with this method. This method lacks a resonance condition, unlike the use of a single AC frequency for ion acceleration as in conventional ion trap CID, and thereby provides a 'broadband' means for inducing CID. Dipolar DC in 3D ion traps has also been described in surface-induced dissociation (SID) and DC tomography experiments [20,22,23].

## 2. Experimental

### 2.1. Instrumentation

All experiments were performed on a dual source Finnigan Ion Trap Mass Spectrometer (ITMS, ThermoFinnigan Corp., San Jose, CA), modified to allow for ion/ion reactions as previously described (Fig. 1) [24]. Briefly, ions from one of two sources can be injected axially and sequentially into the ion trap by means of a DC turning quadrupole. The injection and timing are controlled using Ion

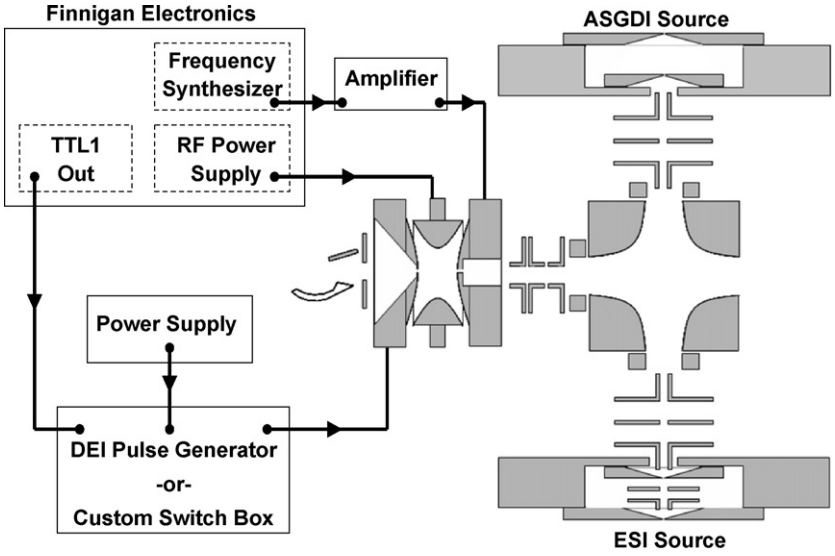


**Fig. 1.** Schematic diagram (not to scale) of the modified dual source 3D ion trap mass spectrometer [25].

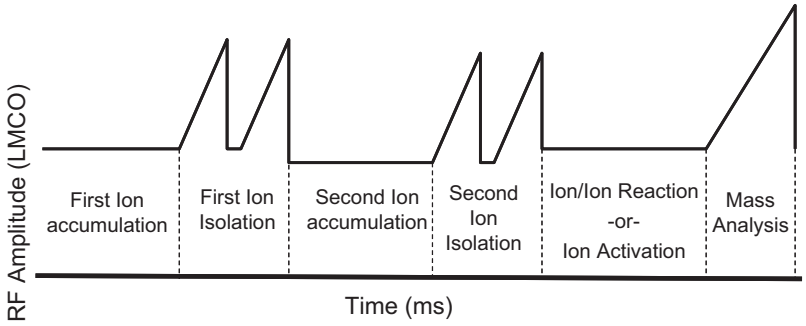


**Fig. 2.** Example of a timing diagram for a tandem mass spectrometry experiment that shows a trace of the relative amplitude of the RF voltage applied to the ring electrode as a function of time. This diagram indicates the temporal locations of the various steps in the process. Other synchronized events (see text), such as the application of supplementary AC and DC voltages, are not shown.

Catcher Mass Spectrometer software (ICMS Ion Trap Software ver. 2.20, University of Florida). Typically, the ion trap is operated by applying the drive RF to the ring electrode with any supplemental AC being applied, 180° out-of-phase, to both the entrance and exit end-cap electrodes. For this work, unless otherwise noted, the AC lead on the exit end-cap was replaced with a DC lead. Application of the manually adjustable ±DC voltage during a scan function was controlled via a transistor-transistor logic (TTL) logic trigger in the system software and either a DEI pulse generator (PVX-4150 model, Directed Energy, Inc., IXYS Colorado) or a home built switchbox. Since the supplemental AC waveform is applied to only one end-cap, the amplitude was increased by a factor of two when used (e.g., during resonance ejection). This resulted in performance comparable to that of the normal mode of operation, whereby 180° out-of-phase sine waves are applied to the end-cap electrodes. Positively charged ions were generated via nanoelectrospray ionization (nESI). Negatively charged ions were generated by atmospheric-sampling glow discharge ionization (ASGDI) [25].

Fig. 2 shows an example of a timing diagram for an ion trap experiment that plots the relative amplitude of the RF amplitude applied to the ring electrode as a function of time. Dual ramps of the RF amplitude in the ion isolation periods represent the use of resonance ejection to eject sequentially ions of lower and higher mass-to-charge than those of interest [26]. Studies monitoring injection efficiency were performed by triggering a repulsive DC voltage on during ion injection. Typical injection times ranged from 20 to 100 ms. Experiments monitoring ejection efficiency were performed by triggering an attractive DC voltage on during mass analysis. Mass analysis was achieved by resonance ejection during an RF amplitude scan at a frequency which gave the desired mass range [27]. Typical mass analysis scan segments were 30 ms. Ion activation was performed by triggering a repulsive DC voltage on during a defined activation period. Activation times varied from 1 to 20 ms. Ion isolations and ion/ion reactions were performed under the influence of varying magnitudes and polarities of monopolar DC, as was dictated by the characteristic under investigation. Ion isolations were performed in 20 ms scan segments. Ion/ion reaction periods typically varied from 50 to 150 ms.

### 2.2. Simulations

A home-written ion trajectory simulation tool has been used. The electric field inside the ion trap was first solved in Comsol (Comsol, Burlington, MA) by using the finite element method. The electric field was then exported to an ion trajectory simulator which solves Newton's equation using 4th order Runge Kutta integration. Langevin's collision theory was used here to model the ion-neutral collision probabilities. The momentum transfer between the ion and target atom resulting from collisions was calculated based on an elastic collision model.

### 2.3. Materials

Bovine ubiquitin, melittin from honey bee venom, bromoisoquinoline, perfluorodimethylcyclohexane (PDCH), and leucine enkephalin were all purchased from Sigma Aldrich (St. Louis, MO). Acetic acid and methanol were purchased from Mallinckrodt (Phillipsburg, NJ). Ubiquitin, melittin, and leucine enkephalin stock solutions of 1.0 mg/mL were prepared in 50:50:1 methanol/water/acetic acid solutions. The bromoisoquinoline stock solution of 1.0 mg/mL was prepared in a 50:50 methanol/water solution. Stock solutions of Ubiquitin, melittin, leucine enkephalin, and 5-bromoisoquinoline were diluted approximately 10-fold prior to nESI. Head-space vapors obtained from a loosely capped bottle of PDCH were mixed with lab air drawn into the ASGDI source.

## 3. Results and discussion

### 3.1. Ion accumulation

Capture efficiency experiments were performed by applying a repulsive DC potential to the exit end-cap during ion accumulation. Ion abundance increases of 2–4-fold were observed (Fig. 3), depending upon injection conditions. The signal intensities of both ubiquitin cations, generated by nESI, and PDCH anions, generated by ASGDI, were increased by factors of about 2.2 when the repulsive DC potential was applied during ion injection in the experiments of Fig. 3. Note that the application of DC to the end-cap electrode had no effect on the observed noise level. Hence, the reported signal increases are reflected by the corresponding improvement in signal-to-noise ratio. The repulsive DC potential acts to decelerate injected ions, presumably increasing the time ions spend in the ion trap and thereby increasing the probability for collisions to remove excess kinetic energy. The enhancement in ion accumulation efficiency has been noted for a wide range of ions formed via nESI and ASGDI suggesting the general nature of this effect.

Fig. 4a compares simulations for the injection of positive ions of $m/z$ 1000 with injected kinetic energy of 11.7 eV ±40%, a bath gas pressure of 0.1 mTorr, and $q_z$ = 0.08 with 0 and 10 V applied to the exit end-cap during ion injection. These simulations of the ion accumulation experiment, which show an optimum range of phase angles for ion trapping that is consistent with previous simulation studies [2,28], indicate that ions are captured over a similar range of the RF phase but with higher efficiency with an optimized DC voltage present on the exit end-cap than in the absence of repulsive DC applied to the exit end-cap. The simulations also show an optimal range for the magnitude of the repulsive DC potential which roughly agrees with experimental observations (Fig. 4b). In this particular case, the simulations for ions of $m/z$ 1000 show optima

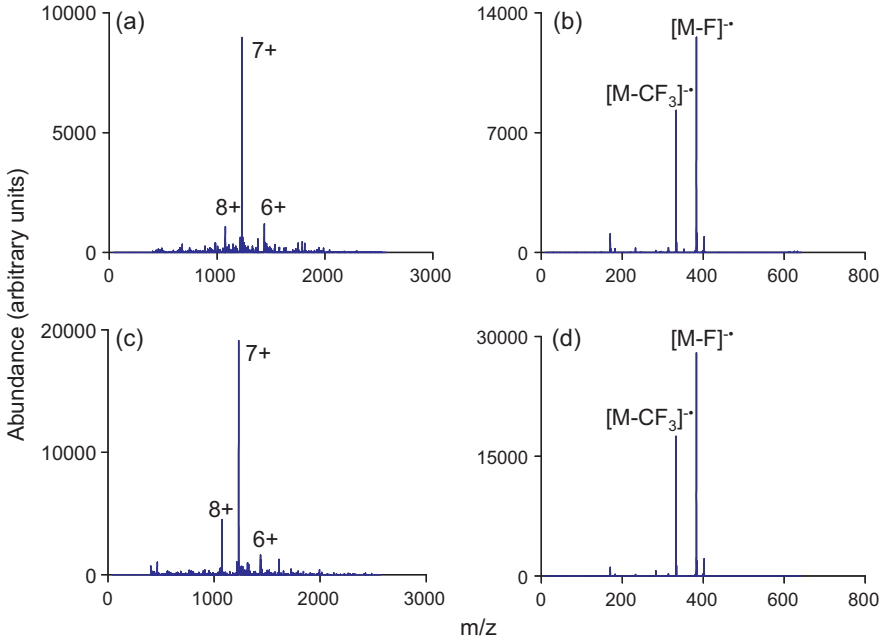


**Fig. 3.** The abundances of ubiquitin cations generated via nESI injected at a $q_z$ of approximately 0.096 (for the 7+ charge state) in the absence of DC (a) and in the presence of +11.5 $V_{DC}$ (b), which shows a roughly 2.2-fold increase. PDCH anions generated via ASGDI injected at a $q_z$ of approximately 0.070 (for $[M-F]^{-\bullet}$) in the absence (c) and presence (d) of −3.5 $V_{DC}$, which shows a similar change in response.

near +10 V, which is similar to the experimentally observed optima noted in the experiments with the ubiquitin ions. However, the simulations underestimate the magnitude of the relative increase in ion accumulation efficiency when compared with experimental data (i.e., they do not show increases of factors of 2–4). The difference in capture efficiency between 'DC on' and 'DC off' modes in the simulations was sensitive to variables such as the $q_z$ value. Under some conditions, for example, differences as large as factors of 4–6 were obtained.

### 3.2. Mass analysis

By applying an attractive DC potential to the exit end-cap during the mass analysis step, an up to 2-fold increase in signal intensity can be observed, as illustrated in Fig. 5 for ions derived from protonated bromoisoquinoline. This phenomenon was consistently observed with a wide range of ions and is interpreted as resulting from the preferential ejection of ions through the exit end-cap by shifting the ion cloud in the direction of the exit end-cap. The application of a repulsive potential to the exit end-cap of equal magnitude resulted in the total loss of signal (data not shown). Preferential ion ejection via one end-cap using mass analysis via resonance ejection has been demonstrated previously via the incorporation of a hexapolar field component and the selection of an appropriate resonance frequency for ejection [29,30]. Such methods also have been shown to give rise to faster ejection, thereby enabling high scan rates. The application of a small attractive DC voltage, as described here, is not expected to alter significantly the ejection rate. However, the effect of uni-directional ejection using this approach is independent of ejection frequency, which allows for flexibility in the selection of the resonance ejection frequency for mass range extension. The electronics used for these studies did not allow for the application of different amplitudes and polarities of DC to the exit end-cap during the course of a single scan function. However, given that ion capture during injection and ion ejection are independent processes, it is expected that application of a repul-

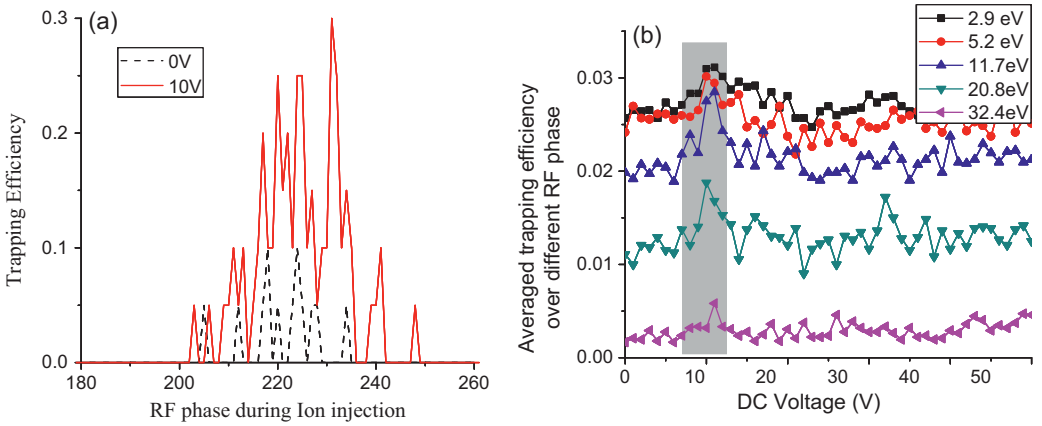


**Fig. 4.** Simulations showing (a) that ion capture is more efficient over similar RF phase (in degrees) in the presence of 10 $V_{DC}$ when compared to 0 $V_{DC}$ ($q_z$ = 0.08, pressure = 0.1 mTorr) and (b) that ion capture efficiency (averaged over the entire RF cycle) for ions with ions of various values of initial kinetic energies is maximized in a common range of repulsive monopolar DC potentials, as indicated by the shaded box ($q_z$ = 0.2, pressure = 0.1 mTorr).

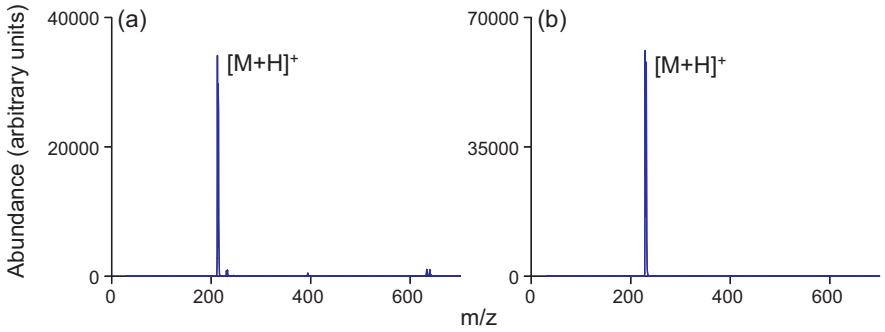


**Fig. 5.** Mass spectra showing the ion signal abundance of bromoisoquinoline cations: (a) in the absence of a DC potential applied to the exit end-cap electrode and (b) in the presence of −18 V applied to the exit end-cap electrode.

sive DC during ion accumulation and an attractive DC during ion ejection could result in signal intensity improvements of 4–8-fold over the equivalent experiment without use of supplementary DC.

### 3.3. Ion isolation

Ion isolation in 3D ion traps can be performed by applying tailored waveforms or by scanning the trapping RF amplitude while simultaneously applying an AC waveform to the end-caps [31]. Low mass ions are ejected by bringing them through the exclusion limit ($q_z = 0.908$) while a range of high mass ions is swept out of the ion trap by resonance ejection. A window of masses that lie between the end of the range of masses swept out by the RF and the onset of the range of ions ejected by resonance ejection is retained in the trap. Alternatively, if the RF amplitude cannot be raised high enough to eject all of the ions on the low mass side of the isolation window, sequential RF ramps that employ different AC frequencies can be used [27]. The amplitude of the supplemental AC must be sufficiently high to eject ions. However, off resonance power absorption, which increases with AC amplitude, can degrade resolution and/or lead to CID of the ions of interest. Therefore, it is desirable to employ the minimum AC amplitude necessary to eject ions. The evidence for uni-directional ion ejection described above implies that the application of a small monopolar DC potential could allow for resonance ejection in an ion isolation step using lower AC amplitudes than the equivalent process without monopolar DC. Fig. 6, which shows results for ion isolation experiments involving the isotopes of protonated bromoisoquinoline, illustrates this point. Fig. 6a and b illustrates the isolation of the protonated $^{79}$Br isotope using a resonance ejection amplitude of 5 $V_{p\text{-}p}$ and no supplemental DC on an end-cap. Fig. 6c shows the result using a resonance ejection amplitude of 3.5 $V_{p\text{-}p}$ and +35 V on the exit end-cap while Fig. 6d shows the result with a resonance ejection amplitude of 3.5 $V_{p\text{-}p}$ and no DC applied to an end-cap. The isolation shown in Fig. 6c is, based on the higher signal intensity of the low mass/charge ratio ion and the lower signal intensity of the high mass/charge ratio ion, better than that shown in Fig. 6b. In the absence of the DC, however, 3.5 $V_{p\text{-}p}$ is insufficient for removal of the $^{81}$Br isotope.

### 3.4. Ion/ion reaction control

The ion/ion reaction period in a 3D ion trap is typically defined imprecisely due to the range of times required for admission of the second reactant ion population and the fact that the oppositely charged ions can react during this period. It is desirable to be able to minimize the reactant ion overlap during this ion accumulation period so that the reaction time can be defined more precisely. The application of a monopolar DC potential can pro-

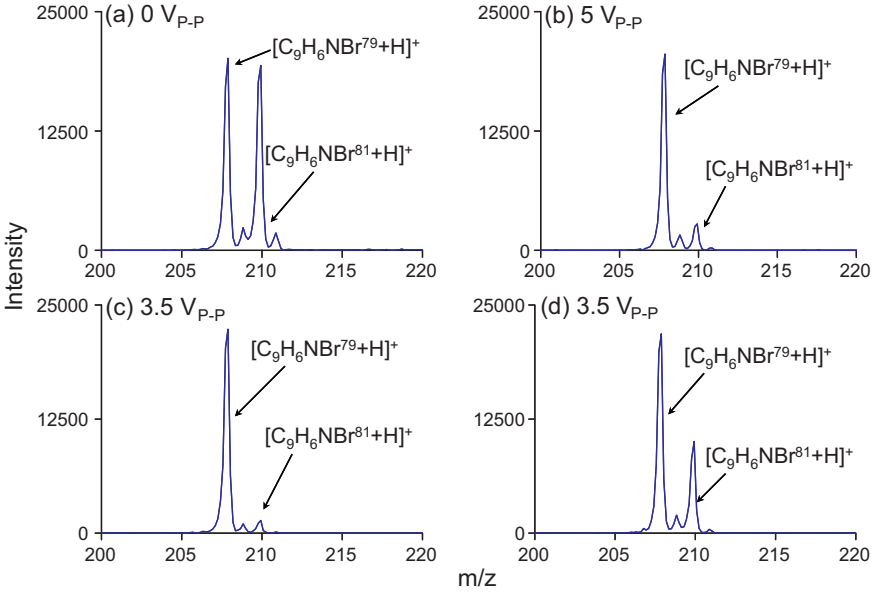


**Fig. 6.** (a) Protonated bromoisoquinoline ions in the absence of any monopolar DC or resonance ejection isolation. (b) Post-ion isolation in the absence of a DC potential using a 5 $V_{p\text{-}p}$ ejection amplitude. (c) Post-ion isolation performed in the presence of +35 $V_{DC}$ and a 3.5 $V_{p\text{-}p}$ ejection amplitude. (d) Ion isolation in the absence of any DC using a 3.5 $V_{p\text{-}p}$ ejection amplitude.

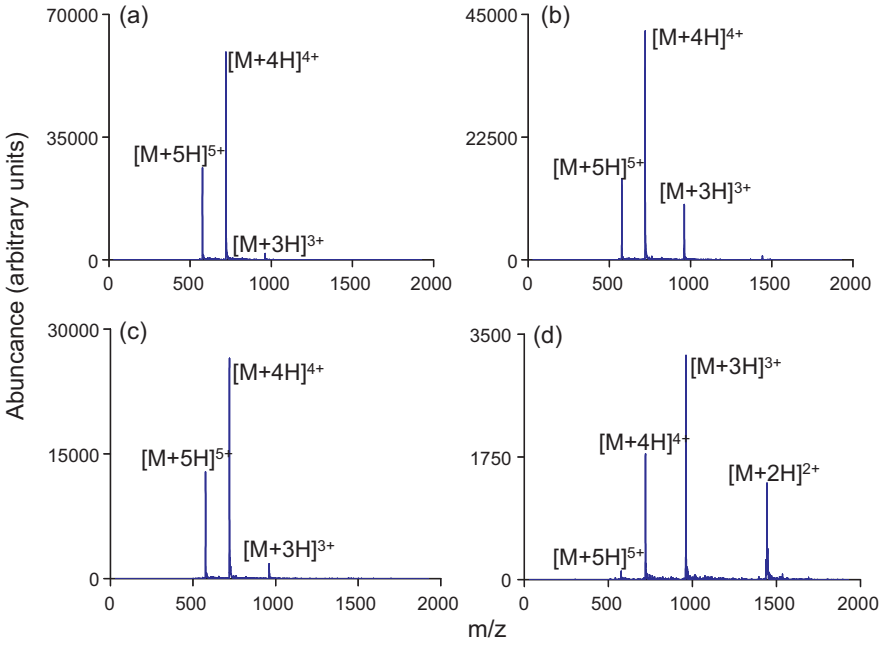


**Fig. 7.** Spectra showing melittin cations prior to (a) and after (b) ion/ion reaction with PDCH anions. Application of $-7\,V_{DC}$ during anion injection and reaction time (c) effectively prevents the ion/ion reaction from proceeding. Application of $-7\,V_{DC}$ during anion injection time only (d) increases the capture efficiency of the reagent anions, increasing their number density in the trap, which allows the charge reduction reaction to proceed further during the set reaction time.

vide a degree of control over the overlap of oppositely charged ions during ion accumulation periods and thereafter. An illustration of this effect is provided in the data of Fig. 7. Initially, melittin cations were injected into the ion trap. Anions derived from glow discharge ionization of PDCH, predominantly the $M^{-\bullet}$, $(M-F\bullet)^{-}$, and $(M-CF_2)^{-\bullet}$ ions, were then injected into the ion trap in both the presence and in the absence of $-7\,V_{DC}$ applied to the exit end-cap. Following the ion accumulation steps and a defined reaction period of 150 ms, the trapping RF amplitude was ramped in order to eject the PDCH anions from the trap prior to mass analysis of the cations [32]. The charge reduction reaction can be quantified in terms of the abundance-weighted average charge state ($q_{average}$), defined as follows:

$$q_{average} = \frac{\sum_i^N (q_i W_i)}{\sum_i^N W_i} \quad (1)$$

where $N$ is the number of observed charge states, $q_i$ is the charge of the $i$th charge state, and $W_i$ is ion abundance of the $i$th charge state [33]. When no anions were admitted into the ion trap, $q_{average}$ was 4.3 (see Fig. 7a). When −7 V DC was applied to the exit end-cap during the anion accumulation period as well as during the reaction period, $q_{average}$ remained at 4.3 (Fig. 7c). In the absence of any DC, $q_{average}$ changed to 4.1 (Fig. 7b). When the −7 V DC was applied only during the anion accumulation period, $q_{average}$ shifted to 3.4 (Fig. 7d). The greater extent of reaction noted in the experiment of Fig. 7d relative to that of Fig. 7b is due to the increased ion accumulation efficiency for the PDCH anions when a repulsive potential is present on the exit end-cap (see above). In this case, the end-cap DC voltage both increased anion accumulation efficiency and minimized the overlap of oppositely charged ions.

To demonstrate that control over ion cloud overlap could be effected during the reaction period, a series of three reaction periods was used following sequential injection of melittin cations and PDCH anions into the ion trap (see Fig. 8). During each reaction period, monopolar DC could be triggered on or off. In these experiments, DC was always on during anion injection in order to prevent data from being complicated by varying degrees of anion injection efficiency. Initially, $-7\,V_{DC}$ was applied during all three periods, preventing the charge reduction reaction and giving an average charge state of 4.3, which was the same as that noted in the absence of anion injection. Removing DC from the first reaction period allowed the ion/ion reaction to proceed to an average charge state of 4.1. Removing DC from the first and third reaction periods resulted in further progression of the reaction, to an average charge state of 3.7. This suggests that the DC could be used to interrupt the progress of the reaction without the loss of reactants such that the reactions could resume upon removal of the DC. Removing DC from all three reaction periods allowed the ion/ion reaction to proceed the furthest, to an average charge state of 3.5.

The mass-to-charge-dependent well-depths, as defined by the trapping conditions, are important to consider when applying DC potentials. Ion/ion reactions between ubiquitin cations and PDCH anions in the presence of lower magnitude DC potentials (less than −7 V) have shown some progression of the charge reduction reaction, thereby demonstrating a type of parallel ion parking (data not shown). Briefly, ubiquitin cations undergo charge reduction reactions to larger mass-to-charge ratios and, under the same trapping conditions, experience shallower trapping wells. As such, the lower charge state/higher $m/z$ cations are shifted further from the trap's geometric center in the $z$ axis by the applied DC, thereby reducing their overlap with the PDCH anions and reducing the ion/ion reaction rate.

### 3.5. DC CID

Pulsed dipolar DC can be used to induce CID in ion traps. Previous reports of pulsed DC CID in 3D traps utilized only short (several microseconds to 1 ms) DC pulses, pulse trains, or slow AC designed to change the physical positions of the ions in the pseudo-potential well inside the trap [19–21]. In this work, a DC potential was applied to an end-cap electrode continuously for periods of two to hundreds of milliseconds. This experiment is analogous to those of Tolmachev et al. with a linear ion trap because the time scales of activation, the magnitudes of the DC, and the LMCO values (well depth) are similar and have all been found to be important variables [15]. Collisional activation arising from the continuous application of monopolar DC

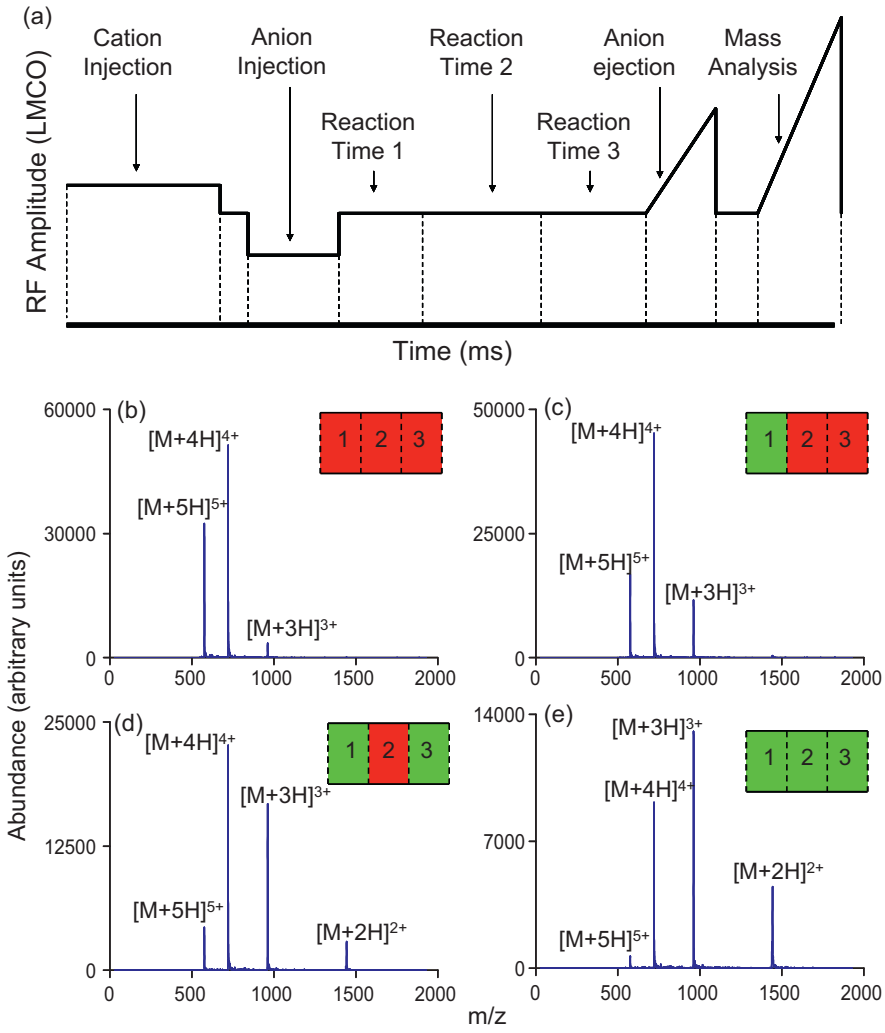


**Fig. 8.** (a) Timing diagram (relative RF amplitude applied to the ring-electrode as a function of time) showing the use of three distinct ion/ion reaction periods during which monopolar DC can be turned on or off, (b) spectra showing ion/ion reactions of melittin cations with PDCH anions using −7 $V_{DC}$ during all three reaction periods, (c) off during the first reaction period and on during the second and third reaction periods, (d) off during the first and third reaction periods and on during the second reaction period, and (e) off during all three reaction periods.

is not expected to result from the initial ion acceleration associated with moving ions away from the ion trap center. Rather, activation is expected to arise from the RF heating mechanism proposed by Tolmachev. That is, ions are moved and held at a location where the RF field is significant, unlike at the ion trap center, where they can undergo acceleration from the main RF applied to the ring-electrode.

Protonated leucine enkephalin, a widely studied model peptide ion [34], is used here to illustrate DC CID in a 3D ion trap. Fig. 9 illustrates the effect of activation time. After isolation of the precursor ion, a potential of +52 V was applied to the exit end-cap while maintaining a low mass cut-off of $m/z$ 100 for activation times ranging from 1 to 20 ms. Fragmentation is noted to begin in as little as 1 ms by the appearance of the $b_4$ and $a_4$ ions. As time is increased, the precursor ion abundance decreases monotonically and the product ion spectrum evolves to show increasingly extensive fragmentation with the appearance of products from sequential fragmentation. Unlike conventional ion trap CID, which employs single frequency resonance excitation, the first (and subsequent) generation product ions generated by DC CID are also subjected to ion acceleration and CID. In conventional ion trap CID, first generation product ions are not subjected to ion acceleration such that longer ion activation times tend not to result in significant changes in relative product ion abundances. The DC CID experiment is expected to be a slow heating process [35] with analogy to infra-red multi-photon dissociation (IRMPD) in which product ions are also exposed to irradiation such that product ion spectra can show significant evolution to more extensive fragmentation with extended activation times.

Ion activation and deactivation rates are comparable with slow heating methods such that precursor ions assume Boltzmann or truncated Boltzmann distributions. The ions therefore can be characterized by an 'effective temperature'. The observed dissociation rate is determined by the effective temperature and the kinetic stability of the ion. The data of Fig. 9 reflect results for a precursor ion of fixed effective temperature with varying times over which the reactions can occur. The effective temperature in the DC CID experiment can be varied by the DC amplitude. This is illustrated in Fig. 10, which shows data for a fixed activation time (1 ms) with various DC amplitudes at a low mass cut-off of $m/z$ 100. Note that the data illustrated in Figs. 9 and 10 were not all collected at a single sitting. Therefore, it is not appropriate to assess MS/MS efficiency from that data. However, as with CID with resonance excitation, there is a competition between ion ejection and ion dissociation. At low DC levels, there appears to be little ion loss whereas ion loss becomes competitive at higher DC levels. The relationship between DC level

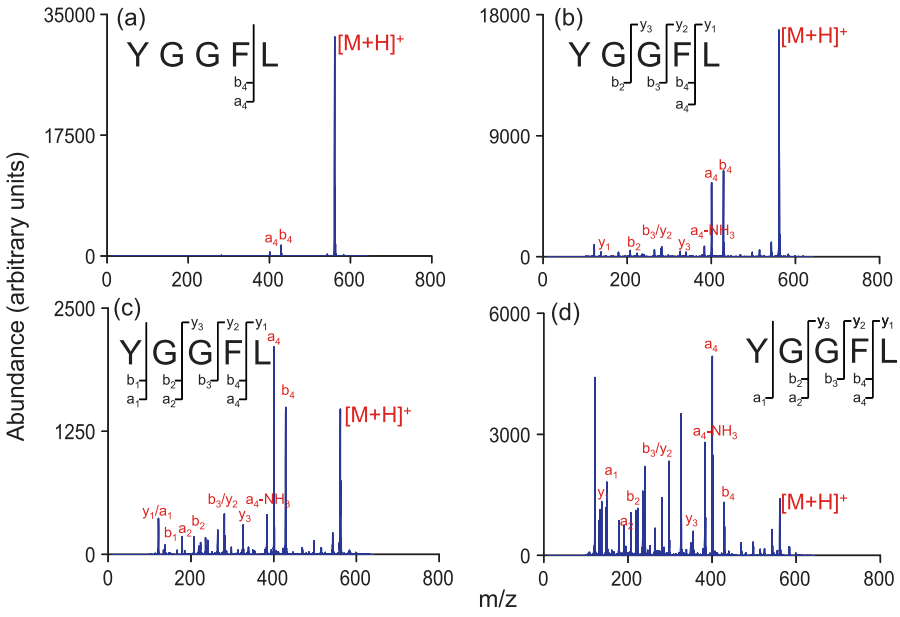


**Fig. 9.** +52 $V_{DC}$ CID of leucine enkephalin with activation times of (a) 1 ms, (b) 5 ms, (c) 10 ms, (d), and 20 ms at a LMCO of *m*/*z* 100.

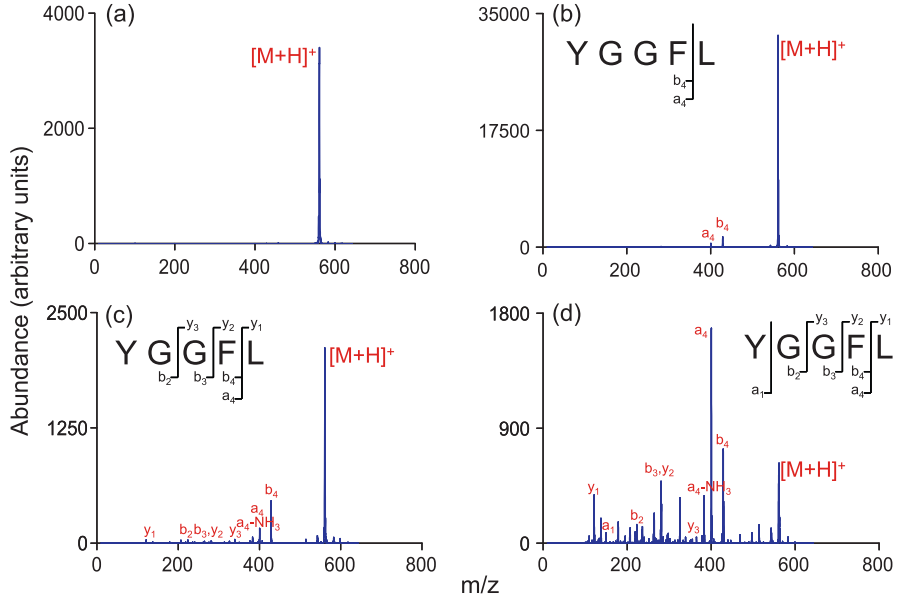


**Fig. 10.** Leucine enkephalin (a) without activation and 1 ms CID of leucine enkephalin with activation potentials of (b) +52.0 $V_{DC}$, (c) +64.3 $V_{DC}$, and (d) +71.2 $V_{DC}$ at a LMCO of *m*/*z* 100.

and MS/MS efficiency as a function of well-depth, as well as a number of other characteristics of DC CID, are currently undergoing systematic investigation.

## 4. Conclusions

A DC potential applied to the exit end-cap electrode of a 3D ion trap can provide useful capabilities in a variety of processes associated with an $MS^n$ experiment. Ion accumulation in the presence of repulsive DC potential has yielded a 2–4-fold increase in capture efficiency. Ion ejection in conjunction with an attractive DC potential resulted in abundance increases of up to a factor of two. Ion isolation via resonance ejection could be effected with lower amplitudes in the presence of monopolar DC, which may be useful when off resonance heating is a problem. Monopolar DC provides a degree of control over the extent of overlap between ion populations of opposite charge. This provides some control over ion/ion reaction rates and can be used to minimize reactions during the second ion accumulation step in an ion/ion reaction experiment as well as for ion parking, the latter having been illustrated previously elsewhere [12]. The application of a DC voltage to an end-cap can also lead to CID, as has already been demonstrated with a linear ion trap. The DC CID approach, like conventional single frequency ion trap CID, is a slow heating method but it is not mass-selective and also leads to activation of product ions. The latter characteristics make it complementary to conventional ion trap CID.

Further studies are under way to fully characterize the strengths and limitations of DC CID in a 3D ion trap. Electronics modifications are also expected to enable better exploitation of the advantages of monopolar DC discussed here. Current instrumentation limits the applied monopolar DC potential to a single polarity and magnitude for any single experiment. Incorporation of flexible software con-

trol of the DC magnitude and polarity in addition to control over its temporal application would enable all of the various capabilities illustrated here to be used in a single $MS^n$ experiment.

## Acknowledgements

Jim Zimmerman, Bob Santini, and Rob Oglesbee of the Jonathan Amy Facility for Chemical Instrumentation are acknowledged for their support. This work was sponsored by the National Institutes of Health under grant no. GM45372.

## References

[1] R.E. March, J.F.J. Todd, Quadrupole Ion Trap Mass Spectrometry, 2nd ed., John Wiley & Sons, Inc., Hoboken, NJ, 2005.
[2] C. Weil, M. Nappi, C.D. Cleven, H. Wollnik, R.G. Cooks, Rapid Commun. Mass Spectrom. 10 (1996) 742.
[3] G.E. Reid, J.M. Wells, E.R. Badman, S.A. McLuckey, Int. J. Mass Spectrom. 222 (2003) 243.
[4] Inventors: M.A. Park, M. Schubert, J. Franzen, Assignee: Bruker Daltonik GMBH, US Patent Application #20090032700.
[5] R.E. March, J.E. Fulford, Ion withdrawal studies of the quadrupole ion trap (QUISTOR). Part I. Characterization of the magnitude of the ion trapping potential well and the location of extractable ions, Int. J. Mass Spectrom. Ion Phys. 30 (1979) 39–55.
[6] Inventor: K. Eizo, Shimadzu Res Lab Europe Ltd., US Patent 6,380,666, Issued on April 30, 2002.
[7] S.M. Michael, B.M. Chien, D.M. Lubman, Anal. Chem. 65 (1993) 2614.
[8] Y. Zerega, P. Perrier, M. Carette, G. Brincourt, T. Nguema, J. Andre, Int. J. Mass Spectrom. 190–191 (1999) 59.
[9] Z. Ouyang, E.R. Badman, R.G. Cooks, Rapid Commun. Mass Spectrom. 13 (1999) 2444.
[10] S.A. McLuckey, J.L. Stephenson Jr., Mass Spectrom. Rev. 17 (1998) 369.
[11] S.J. Pitteri, S.A. McLuckey, Mass Spectrom. Rev. 24 (2005) 931.
[12] Inventors: P.B. Grosshans, C.M. Ostrander, C.A. Walla, Assignee: Hitachi High Technologies America, Inc. (San Jose, CA), US Patent 6,674,067, Issued on January 4, 2004.
[13] S.A. McLuckey, G.E. Reid, J.M. Wells, Anal. Chem. 74 (2002) 336.
[14] P.A. Chrisman, S.J. Pitteri, S.A. McLuckey, Anal. Chem. 78 (2006) 310.
[15] A.V. Tolmachev, A.N. Vilkov, B. Bogdanov, L. Păsa-Tolić, C.D. Masselon, R.D. Smith, J. Am. Soc. Mass Spectrom. 15 (2004) 1616.
[16] J.N. Louris, R.G. Cooks, J.E.P. Syka, P.E. Kelley, G.C. Stafford Jr., J.F.J. Todd, Anal. Chem. 59 (1987) 1677.
[17] M. Wang, J.E. George III, Technology progress and application in GC/MS and GC/MS/MS, in: R.E. March, J.F.J. Todd (Eds.), Practical Aspects of Trapped Ion Mass Spectrometry, vol. V, CRC Press, Boca Raton, FL, 2009 (Chapter 15).
[18] C. Paradisi, J.F.J. Todd, U. Vettori, Org. Mass Spectrom. 27 (1992) 251.
[19] W.R. Plass, Int. J. Mass Spectrom. 202 (2000) 175.
[20] S.A. Lammert, R.G. Cooks, Rapid Commun. Mass Spectrom. 6 (1992) 528.
[21] M. Wang, S. Schachterle, G. Wells, J. Am. Soc. Mass Spectrom. 7 (1996) 668.
[22] S.A. Lammert, R.G. Cooks, Rapid Commun. Mass Spectrom. 2 (1991) 487.
[23] R.G. Cooks, C.D. Cleven, L.A. Horn, M. Nappi, C. Weil, M.H. Soni, R.K. Julian, Int. J. Mass Spectrom. Ion Process. 146–147 (1995) 147.
[24] J.M. Wells, P.A. Chrisman, S.A. McLuckey, J. Am. Soc. Mass Spectrom. 13 (2002) 614.
[25] S.A. McLuckey, G.L. Glish, K.G. Asano, B.C. Grant, Anal. Chem. 60 (1988) 2220.
[26] S.A. McLuckey, D.E. Goeringer, G.L. Glish, J. Am. Soc. Mass Spectrom. 2 (1991) 11.
[27] R.E. Kaiser, R.G. Cooks, G.C. Stafford, J.E.P. Syka, P.H. Hemberger, Int. J. Mass Spectrom. Ion Process. 106 (1991) 79.
[28] S.T. Quarmby, R.A. Yost, Int. J. Mass Spectrom. 190–191 (1999) 81.
[29] J. Franzen, R.-H. Gabling, M. Schubert, Y. Wang, in: R.E. March, J.F.J. Todd (Eds.), Practical Aspects of Ion Trap Mass Spectrometry, vol. I, CRC Press, Boca Raton, FL, 1995 (Chapter 3).
[30] M. Splendore, E. Marquette, J. Oppenheimer, C. Huston, G. Wells, Int. J. Mass Spectrom. 190–191 (1999) 129.
[31] J.N. Louris, J.S. Brodbelt-Lustig, R.G. Cooks, G.L. Glish, G.J. Van Berkel, S.A. McLuckey, Int. J. Mass Spectrom. Ion Process. 96 (1990) 117.
[32] J.L. Stephenson Jr., S.A. McLuckey, Anal. Chem. 69 (1997) 3760.
[33] A.T. Iavarone, J.C. Jurchen, E.R. Williams, Anal. Chem. 73 (2001) 1455.
[34] J. Sztáray, A. Memboeuf, L. Drahos, K. Vékey, Mass Spectrom. Rev. (2010), doi:10.1002/mas.20279.
[35] S.A. McLuckey, D.E. Goeringer, J. Mass Spectrom. 32 (1997) 461.